Electrochimica Acta 56 (2011) 5080–5084

Contents lists available at ScienceDirect

Electrochimica Acta

journal homepage: www.elsevier.com/locate/electacta

Nitrogen-doped carbon nanotubes as air cathode catalysts in zinc-air battery

Shaomin Zhu[a,b], Zhu Chen[b], Bing Li[b], Drew Higgins[b], Haijiang Wang[c], Hui Li[c], Zhongwei Chen[b,*]

[a] College of Environmental and Chemical Engineering, Dalian Jiaotong University, Dalian 116028, China
[b] Department of Chemical Engineering, University of Waterloo, Waterloo, ON, N2L 3G1, Canada
[c] Institute for Fuel Cell Innovation, National Research Council Canada, Vancouver, BC, V6T 1W5, Canada

ARTICLE INFO

Article history:
Received 1 February 2011
Received in revised form 21 March 2011
Accepted 21 March 2011
Available online 30 March 2011

Keywords:
Nitrogen-doped carbon nanotubes
Oxygen reduction reaction
Air cathode
Catalysts
Zinc-air batteries

ABSTRACT

Nitrogen-doped carbon nanotubes (N-CNTs) derived from ethylenediamine precursor have been used as air cathode catalyst for zinc-air batteries (ZABs) in half cell and single cell. Investigation of N-CNTs employed a rotating disc electrode system revealed excellent catalytic activity towards oxygen reduction reaction (ORR) in alkaline electrolyte. The influence of alkaline electrolyte concentration on single cell performance of ZABs has also been explored. The highest cell performance was achieved at an electrolyte concentration of 6 M KOH, which resulted in a maximum cell power density of 69.5 mW cm^{-2}.

1. Introduction

The limited supply of fossil fuels, combined with rising environmental concerns from their widespread use has stimulated extensive research into the development of "green" energy sources. Fuel cells, more specifically proton exchange membrane fuel cells (PEMFCs) and direct methanol fuel cells (DMFCs) are considered promising power generation systems that have been extensively investigated, as they can efficiently convert chemical energy into electrical energy while only producing environmentally benign byproducts [1–4]. However, the commercialization of this technology is still hindered by several issues including the high cost and limited availability of noble electrocatalyst materials, hydrogen compression and storage challenges as well as problems arising from methanol crossover. Zinc-air batteries (ZABs) on the other hand have drawn increasing attention in recent years due to their high specific energy, environmental friendliness and low operation risks [5]. Moreover, these devices have the potential to utilize non-precious metal electrocatalyst and cost-effective cell design due to system simplicity, providing immense economical benefits compared with PEMFCs and DMFCs. Thus, ZABs are rapidly emerging as a promising technology for both stationary and mobile applications [5–7].

In principle, ZABs employ a liquid alkaline electrolyte and operate with a steady supply of air. The oxygen in the air will react at the cathode, forming hydroxyl ions that will migrate through the liquid electrolyte to the porous zinc anode. At the anode, the hydroxyl ions will react to form zinc oxide, which is the only one byproduct of ZABs operation. However, several major technical challenges must be overcome at the current status of ZABs development in order to achieve the commercialization of this technology. Specifically, significant issues relating to relatively low performance and insufficient stability of the air-cathode catalyst materials must be resolved. Several laboratories have been engaged in this research, pursuing the development of potential non-precious cathode electrocatalyst materials [5–10]. Metal oxide based catalysts have been most widely investigated, including MnO_2, and materials with spinel and perovskite crystal structures [5,8–10]. Unfortunately, the activity and stability towards ORR are still insufficient for practical application in ZABs. The push for ZABs commercialization continues to stimulate a great deal of interest in the development of alternative cathode catalyst materials for better ORR activity and long term stability in alkaline media.

Recently, nitrogen-doped carbon nanotubes (N-CNTs) have displayed significant ORR activity in acid and alkaline solutions, attributed to the heterogeneous nitrogen doping resulting in ORR active functional groups [11–14]. In our previous work, we have reported that highly active N-CNTs can be synthesized using an ethylenediamine/ferrocene precursor solution, with the resulting materials displaying superior ORR activity under alkaline conditions compared even with traditional platinum based catalyst materials [15–17]. Thus, we have adopted this strategy to utilize highly active N-CNT based materials as air-cathode electrocatalysts in order to improve the performance of ZABs. The physiochemical

* Corresponding author. Tel.: +1 519 888 4567x38664; fax: +1 519 746 4979.
E-mail address: zhwchen@uwaterloo.ca (Z. Chen).

0013-4686/$ – see front matter © 2011 Elsevier Ltd. All rights reserved.
doi:10.1016/j.electacta.2011.03.082

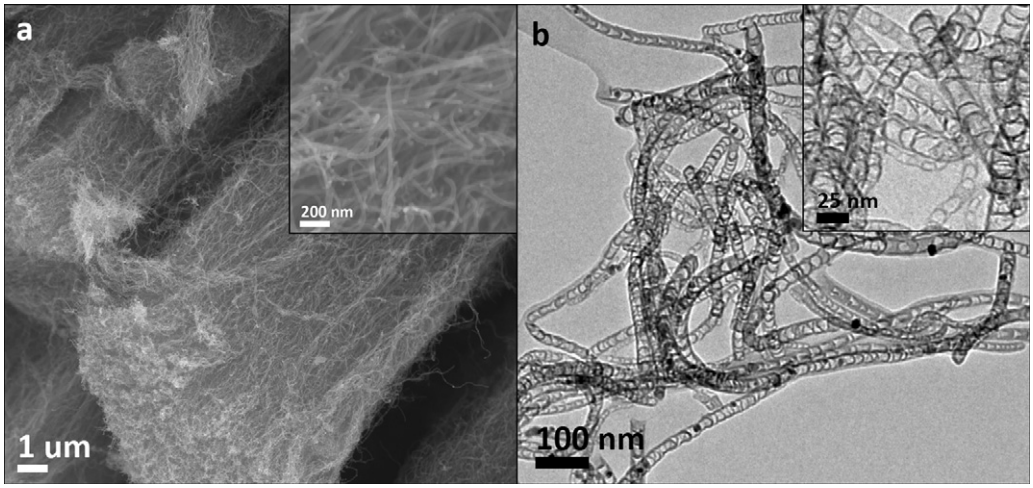

Fig. 1. (a) SEM and (b) TEM images of N-CNTs samples.

properties of N-CNTs were extensively characterized by scanning electron microscopy (SEM) and transmission electron microscope (TEM). Electrochemical catalytic activity of N-CNTs was investigated by linear sweep voltammetry (LSV) using a rotating disc electrode (RDE) system, which confirmed the excellent ORR activity in alkaline condition. Notably, the novelty of this work lies in the utilization of highly active N-CNTs as cathode catalyst materials in a single cell ZABs setup. The single cell performance was investigated using electrochemical impedance spectroscopy (EIS) in different electrolyte concentrations. Utilization of N-CNTs has led to high ZABs performance suggesting the great potential of N-CNTs as high performance catalyst for ORR on the air-cathode of ZABs.

2. Experimental

2.1. Preparation of N-CNT electrocatalysts

N-CNTs were synthesized at 800 °C by chemical vapor deposition (CVD) using a tube furnace setup as described in our previous papers [15,16]. Briefly, ethylenediamine was utilized as the precursor material for nitrogen and carbon, with ferrocene dissolved in the solution as a growth catalyst. The as-prepared N-CNTs were refluxed in 0.5 M H_2SO_4 at 90 °C for 1 h in order to remove any residual iron particles remaining from the growth catalyst. The purified N-CNTs were thoroughly washed with deionized water until the pH value of the filtrate reached 7, and were then dried at 60 °C overnight and collected for further study.

2.2. Catalyst characterization

The morphology of N-CNT electrocatalysts was observed using transmission electron microscopy (TEM) analyses, with a JEOL 2010. The samples were ultrasonically dispersed in ethanol and then dropped into the carbon-coated copper grids prior to the measurements. To image the morphologies of the material, scanning electron microscopy (SEM) micrographs of the surface was performed by LEO FESEM 1530.

2.3. Electrochemical characterization

To investigate the ORR catalytic activity of the samples, a rotating disc electrode (RDE) half-cell setup was used. Catalyst ink was prepared by homogeneously dispersing 4 mg of catalyst in 2 mL of 0.5 wt% Nafion solution containing ethanol and deionized water. The glassy carbon disc working electrode was coated with 20 μL of catalyst ink and allowed to dry to achieve a catalyst loading of 0.2 mg cm^{-2}. A platinum wire counter electrode and a double junction Ag/AgCl reference electrode were utilized in the RDE system. The ORR activity at different working electrode rotation speeds was investigated using linear sweep voltammetry in oxygen saturated 0.1 M KOH. Capacitive current and background readings were obtained using cyclic voltammetry method in nitrogen saturated electrolyte.

2.4. Fabrication of ZABs single cell and performance measurements

ORR performance of the N-CNTs materials in a home-made ZAB was determined using a single cell MEA setup. Catalyst ink was prepared by homogeneously dispersing 9.4 mg of catalytic material in an admixture of isopropanol, 5 wt% Nafion and deionized water. The catalyst ink was sprayed on a commercial gas diffusion layer (Ion Power Inc., SGL Carbon 10 BB, 2.5 cm by 2.5 cm) followed by baking in oven for 1 h at 80 °C. The home-made ZAB single cell was fabricated by sandwiching an electrolyte reservoir (filled with 6 M KOH) with catalyst loading of 0.2 $mg_{catalyst}$ cm^{-2}, and a polished zinc plate anode. Electrochemical impedance spectroscopy was performed from 10 kHz to 0.05 Hz with amplitude of 10 mV using a multichannel potentiostat (Princeton Applied Research, VersaSTAT MC).

3. Results and discussion

SEM images of the N-CNTs were taken to investigate the microstructure of the material as shown in Fig. 1a, where bundles of aligned N-CNTs (30–50 nm diameter) are observed. TEM images presented in Fig. 1b illustrate structural defects in the form of small and round bamboo-like compartments, which are consistently observed with N-CNTs due to the incorporation of nitrogen atoms into the graphitic structure [11–14].

RDE voltammetry was utilized in order to determine the half-cell ORR activity of the N-CNTs in 0.1 M KOH electrolyte. Fig. 2 displays the RDE current–voltage polarization curves obtained at different electrode rotation speeds (100, 400, 900, 1600 and 2500 rpm). N-CNTs displayed excellent catalytic activity as commonly observed with non-precious electrocatalyst materials in alkaline solution [5,8]. The nitrogen content of the N-CNT utilized in this study has a nitrogen content of approximately 4 at.% (determined by X-ray photoelectron spectroscopy which is not

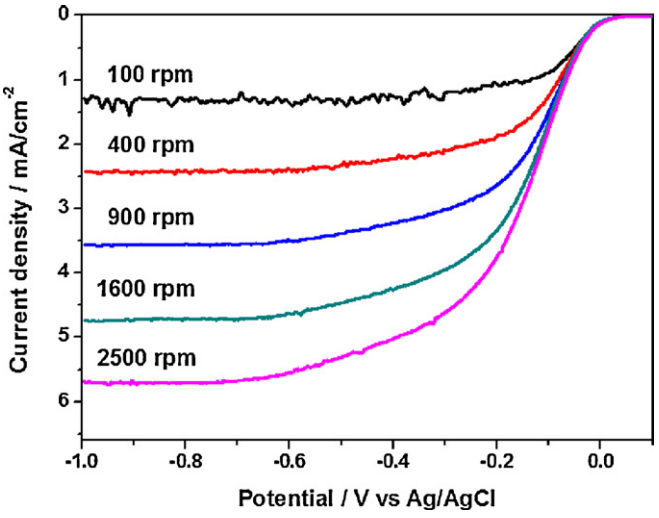

Fig. 2. ORR polarization curves obtained for O_2 reduction in 0.1 M KOH in the cathodic sweep direction at a scan rate of 10 mV s^{-1} and electrode rotation speeds from 100 to 2500 rpm.

shown here). The overall nitrogen content plays an important role in the ORR activity of N-CNT where increase in nitrogen content of the N-CNT has been correlated with higher ORR activity [18]. Furthermore, heterogeneous incorporation of nitrogen atom into the graphitic structure of CNTs leads to the creating of many structural defects which could expose edge and planar sites that facilitate the adsorption of molecule oxygen on catalyst surface for improved ORR activity [15,16]. The ORR polarization curve of N-CNTs coated electrode can be separated into three regions, (1) kinetically controlled region from ca. −0.05 to −0.25 V, (2) combined kinetic-diffusion controlled region from ca. −0.25 to −0.6 V, and (3) mass diffusion controlled region at potentials greater than −0.6 V. For a kinetic-diffusion control process, ORR activity can be analyzed using Koutecky–Levich (K–L) plots. The overall current density can be separated into the diffusion and kinetic contributions by applying the K–L equation [19,20]:

$$\frac{1}{j} = \frac{1}{j_k} + \frac{1}{B\omega^{1/2}} \quad (1)$$

$$B = 0.62nFC(O_2)D_{O_2}^{2/3}\nu^{-1/6} \quad (2)$$

where j is the measured overall current density, j_k is the kinetically limited current density, ω is the rotation speed of the electrode, and B is the Levich slope, the theoretical value of which is given by the Eq. (2). In the Eq. (2), n is the number of electrons transferred in the reaction, F Faraday's constant, D_{O_2} the diffusion coefficient of oxygen (1.86×10^{-5} cm^2 s^{-1}), ν the kinematics viscosity of the electrolyte solution (1.008×10^{-2} cm^2 s^{-1}) and $C(O_2)$ the saturate concentration of oxygen (1.21×10^{-6} mol/L). The values of these coefficients are referring to 0.1 M KOH solution [20].

From the K–L plots (Fig. 3a), the kinetic currents of oxygen reduction can be calculated from the intercepts of the linear K–L relationships. Additionally, the Levich slope and the number of the electrons exchanged in the reduction reaction can be obtained from the slope of the K–L relationships. The K–L plots of the N-CNTs at different electrode rotations for the N-CNTs are presented in Fig. 3a showing linear and parallel characteristics in the kinetic-diffusion controlled region are observed, which indicates first-order ORR kinetics with respect to oxygen. The value of Levich slope is 0.116 mA cm^{-2} $rpm^{-1/2}$ according to the K–L plot, which is in good agreement with the theoretical value of 0.104 mA cm^{-2} $rpm^{-1/2}$ for a four-electron reduction of oxygen in 0.1 M KOH [19]. This indicates four-electron reduction process by N-CNTs making it a promising and effective air-cathode catalyst for ZABs. Fig. 3b presents the Tafel plots for the reduction of oxygen on the N-CNTs coated electrode. Two distinct Tafel regions with different slopes were obtained. The Tafel slope at low current density is −60 mV dec^{-1}, and the Tafel slope at high current density is from −260 to −500 mV dec^{-1}. These results indicate that the ORR kinetics on N-CNTs in alkaline solutions is described by the similar equation in the case of Pt, and the first charge transfer rate is the rate determining step [20]. The existence of two regions with different slopes in the Tafel plots for the N-CNT coated electrode can be explained in terms of the coverage of the electrode surface by adsorbed oxygen species. This coverage follows Temkin and Langmuir isotherm in different current density regions [20,21].

The electrolyte concentration is one of the key factors affecting the ZABs performance. Polarization and power density curves of N-CNTs coated cathode operated in different KOH electrolyte are displayed in Fig. 4. From the figures, improved cell performance is evident with increasing KOH concentrations from 1 to 6 M and reaches the optimal performance at 6 M. The observed trend is attributed to the increase in ionic conductivity of the electrolyte. Moreover, increasing KOH concentration is favorable for the anode reaction according to the Nernst equation. Single cell current density of 24.8, 51.5, and 78.6 mA cm^{-2} was obtained at 0.8 V using 1, 3, and 6 M KOH electrolyte, respectively (Table 1). Similarly, the maximum power density of the ZABs increased from 19.7 to 69.5 mW cm^{-2} when the KOH concentration increased from 1 to 6 M. However, a further increase in KOH concentration from 6 to 12 M did not cause an obvious increase in cell performance. This is attributed to an increase in the solution viscosity and a decrease

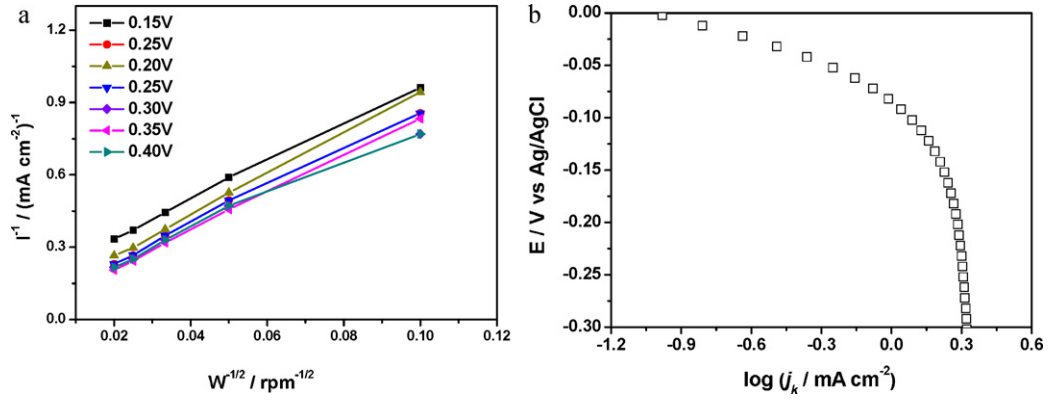

Fig. 3. (a) Koutechy–Levich and (b) Tafel plots for N-CNTs normalized to the electrochemically active surface area for O_2 reduction in 0.1 M KOH solution at a rotating speed of 1600 rpm.

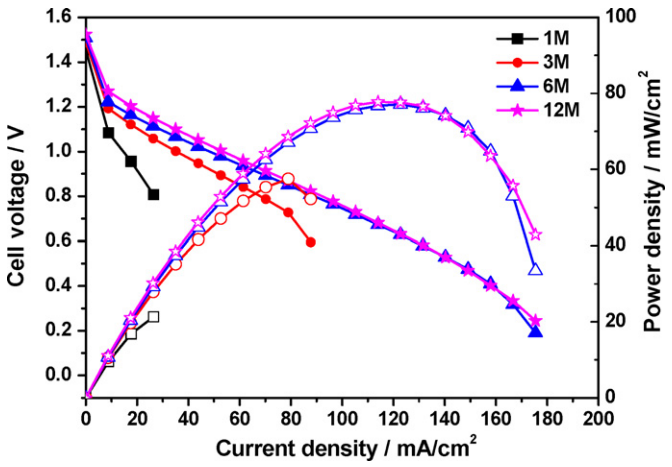

Fig. 4. MEA polarization and power density curves for 0.2 $mg_{catalyst}$ cm^{-2} N-CNTs cathodic catalyst loading in a ZAB single cell system.

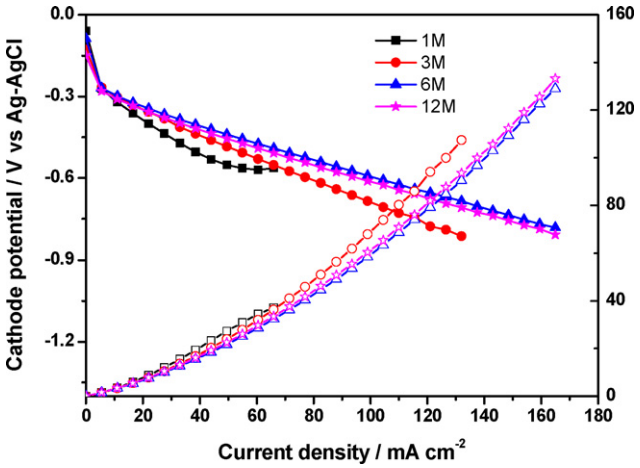

Fig. 5. *In situ* cathodic potential and power density curves for 0.2 $mg_{catalyst}$ cm^{-2} N-CNTs cathodic catalyst loading in a ZAB single cell system.

in the mobility of ions [5,8]. Based on Fig. 4 (or Table 1), using 6 M KOH, which was optimum for the ZABs used for this study.

In order to evaluate the contribution of the cathode catalyst to the overall cell performance, *in situ* cathodic potentials under different KOH concentrations were tested in the ZAB single cell system (Fig. 5). The initial potential of the cathode decreased from −0.036 to −0.144 V vs. Ag/AgCl when the KOH concentration was increased from 1 to 12 M (Table 1). This is mainly attributed to the increasing OH^- concentration at the surface of the cathode taking part in the reaction according to the Nernst equation. The main reason of the difference of cathode potential in ohmic and concentration loss regime is the change in solution conductivity and viscosity arising from different electrolyte concentration. The air-cathodes operating in 6 and 12 M KOH electrolyte showed very similar maximum power density of 129.0 and 133.3 mW cm^{-2}, respectively.

Electrochemical impedance spectroscopy (EIS) was used to investigate the electrochemical reactions affecting the performance of ZABs electrodes. Critical information such as, charge transfer process of the electrochemical reaction, catalyst conductivity as well as electrode porous structure can be determined by EIS. Compared with polarization occurred on the cathode of ZABs, anode polarization is often neglected owing to the smaller magnitude [22,23]. Fig. 6 illustrates the Nyquist plots of the ZABs operated in different electrolyte concentration and battery voltage. The impedance spectra obtained at 1 M KOH show significant deviation from the spectra obtained at higher electrolyte concen-

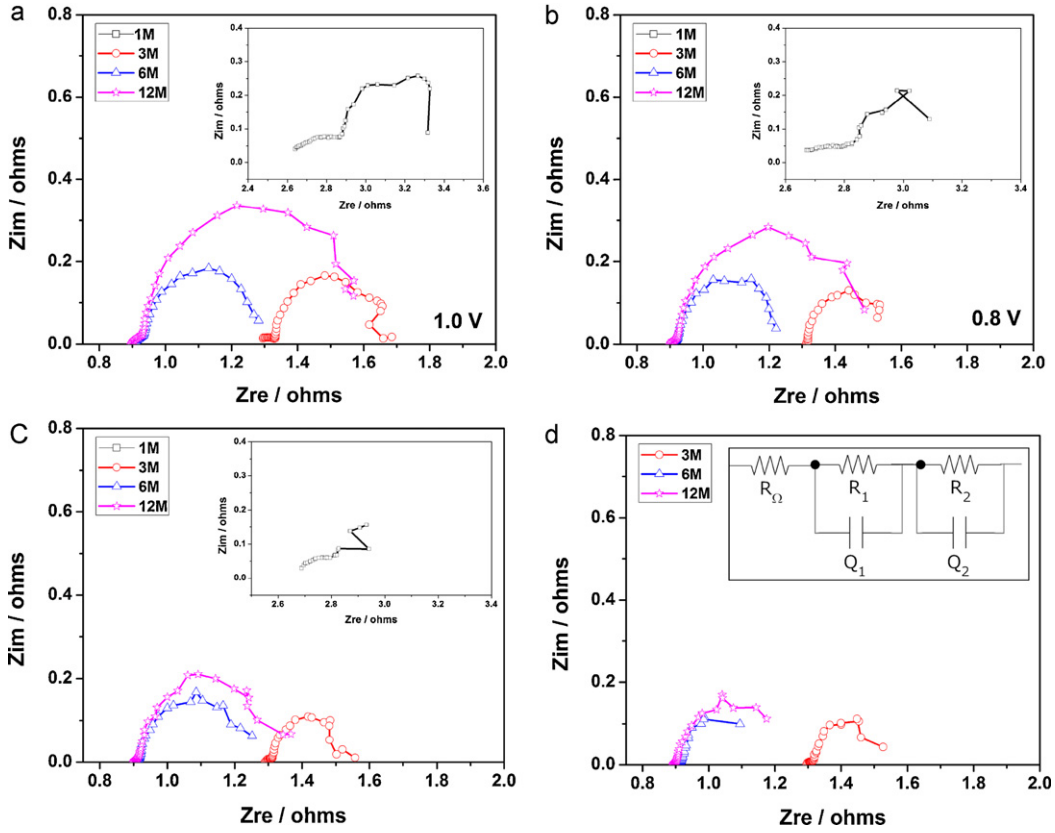

Fig. 6. Nyquist plots of ZAB single cells with N-CNTs catalyst at (a) 1.0, (b) 0.8, (c) 0.6, and (d) 0.4 V. Inset of (d), illustrates the equivalent circuit used to model the impedance data.

Table 1
Oxygen electrode activities.

KOH (M)	OCV (V)	Current density at 0.8 V (mA cm^{-2})	Peak power density (mW cm^{-2})	Cathode potential vs. Ag/AgCl, $I = 0$ (V)	Peak power density of cathode (mW cm^{-2})
1	1.44	24.8	19.7	−0.036	37.2
3	1.43	51.5	46.9	−0.054	107.4
6	1.44	78.6	69.5	−0.084	129.0
12	1.45	78.6	68.8	−0.144	133.3

Table 2
Parameters evaluated from fit of EIS in ZAB single cell mode.

KOH (M)	1.0 V			0.8 V			0.6 V			0.4 V		
	R_Ω	R_1	R_2	R_Ω	R_1	R_2	R_Ω	R_1	R_2	R_Ω	R_1	R_2
1	2.64	0.23	0.67	2.67	0.16	0.42	2.68	0.1	–	–	–	–
3	1.29	0.04	0.38	1.26	0.05	0.27	1.29	0.02	0.27	1.29	0.02	0.24
6	0.91	0.03	0.37	0.91	0.01	0.31	0.91	0.01	0.34	0.91	0.01	0.18
12	0.89	0.04	0.68	0.9	0.02	0.59	0.9	0.01	0.47	0.89	0.01	0.28

tration, which could be caused by the low ionic conductivity of the 1 M KOH electrolyte that hinders the discharge process during ZABs operation. Impedance spectra obtained at high concentration shares similar shape where a depressed arc at high frequency is preceded by a larger semicircle that spans from mid to low frequency. The intercept of the impedance spectra at high frequency with the real axis is denoted R_Ω, representing the internal resistance of the cell including total ohmic resistance which includes resistance arise from the electrolyte, catalyst layer, as well as contact resistances [23]. The equivalent circuit used to fit the data is showed in the inset of Fig. 6d. Through extrapolation of the onset of the semicircle to the real axis, R_1 is obtained. R_1 is strongly related to electrolyte conductivity thus it could reflect the ionic ohmic drop inside the gas diffusion electrode [23,24]. The intercept of the impedance spectra at low frequency with the real axis is denoted R_2, representing the mass-transfer process. Based on the impedance data summarized in Table 2, several trends can be observed with respect to the difference resistances of the equivalent circuit. Under increasing electrolyte concentration continuous decrease in R_Ω is observed as reflected by the shift in the intercept of the impedance spectra with the real axis at high frequency. This phenomenon is expected as R_Ω is correlated with the electrolyte resistance in the ZABs. Similar trend is observed in R_1 where the strong dependence on electrolyte conductivity leads to a decrease in its value with increase in KOH concentration. However, no further decrease in R_1 value was observed when KOH concentration is increased beyond 3 M. It should be noted that the value of R_1 beyond 3 M is rather small which could be influence by the experimental errors to a certain degree. Therefore, the treatment of the value of R_1 beyond 3 M should be approached with caution. Unlike the previously mentioned resistance, R_2 increase alongside with KOH concentration as reflected by the increase in the low frequency semicircle. This effect has been observed by others [24,25] where deeper penetration of the porous electrode by highly concentrated KOH results in limited gas = accessibility which in turn increases mass transport resistance. Further study of the correlation between of cell voltage and the resistance (R_2) reveal a decreasing trend with respect to increasing overpotential, which has been observed previously [26,27].

4. Conclusions

In summary, N-CNTs materials possessing a high activity towards the ORR in alkaline solution were employed as air-cathode electrocatalyst material in a single cell ZAB setup. Moreover, the effect of KOH concentration in the ZAB electrolyte was investigated in order to determine the optimal concentration for cell performance, dependent on the ionic conductivity and viscosity of the liquid electrolyte solution. With an air-cathode catalyst loading of 0.2 mg cm^{-2} and an optimal KOH electrolyte concentration of 6 M, a high cell power density of 69.5 mW cm^{-2} was obtained. The excellent ORR activity and single cell performance strongly suggested that N-CNTs could be promising cathode catalysts for ZAB.

References

[1] P.H. Matter, L. Zhang, U.S. Ozkan, J. Catal. 239 (2006) 83.
[2] M.H. Shao, K. Sasaki, R.R. Adzic, J. Am. Chem. Soc. 128 (2006) 3526.
[3] Y. Shao, J. Sui, G. Yin, Y. Gao, Appl. Catal., B 79 (2008) 89.
[4] V. Neburchilov, H. Wang, J.J. Martin, W. Qu, J. Power Sources 195 (2010) 1271.
[5] Z. Chen, J. Choia, H. Wang, H. Li, Z.W. Chen, J. Power Sources 196 (2011) 3673.
[6] S.W. Eom, C.W. Lee, M.S. Yun, Y.K. Sun, Electrochim. Acta 52 (2006) 1592.
[7] W.K. Chao, C.M. Lee, S.Y. Shieu, C.C. Chou, F.S. Shieu, J. Power Sources 177 (2008) 637.
[8] X.Y. Wang, P.J. Sebastian, M.A. Smit, H.P. Yang, S.A. Gamboa, J. Power Sources 124 (2003) 278.
[9] Y.F. Yang, Y.H. Zhou, J. Electroanal. Chem. 415 (1995) 143.
[10] G.Q. Zhang, X.G. Zhang, Electrochim. Acta 49 (2004) 873.
[11] E.J. Biddinger, D. von Deak, U.S. Ozkan, Top. Catal. 52 (2009) 1566.
[12] P.H. Matter, E. Wang, M. Arias,J.E. Biddinger, U.S. Ozkan, J. Phys. Chem. B 110 (2006) 18374.
[13] V. Nallathambi, J.W. Lee, S.P. Kumaraguru, G. Wu, B.N. Popov, J. Power Sources 183 (2008) 34.
[14] K. Gong, F. Du, Z. Xia, M. Durstock, L. Dai, Science 323 (2009) 760.
[15] Z. Chen, D.C. Higgins, Z.W. Chen, Carbon 48 (2010) 3057.
[16] D.C. Higgins, D. Meza, Z.W. Chen, J. Phys. Chem. C 114 (50) (2010) 21982.
[17] D.C. Higgins, Z. Chen, Z.W. Chen, Electrochim. Acta 56 (2011) 1570.
[18] Z. Chen, D. Higgins, Z. Chen, Carbon 48 (2010) 3057.
[19] X. Li, A.L. Zhu, W. Qu, H. Wang, R. Hui, L. Zhang, J. Zhang, Electrochim. Acta 55 (2010) 5891.
[20] N.R. Elezović, B.M. Babić, Lj.M. Vračar, N.V. Krstajić, J. Serb. Chem. Soc. 72 (2007) 699.
[21] K. Tammeveski, M. Arulepp, T. Tenno, C. Ferrater, J. Claret, Electrochim. Acta 42 (1997) 2961.
[22] V.A. Paganin, C.L.F. Oliveira, E.A. Ticianelli, T.E. Springer, E.R. Gonzalez, Electrochim. Acta 43 (1998) 3761.
[23] G.B. Chen, H.M. Zhang, H.P. Ma, H.X. Zhong, Electrochim. Acta 54 (2009) 5454.
[24] F. Bidault, A. Kucernak, J. Power Sources 195 (2010) 2549.
[25] F. Bidault, D.J.L. Brett, P.H. Middleton, N. Abson, N.P. Brandon, Int. J. Hydrogen Energy 35 (2010) 1783.
[26] M. Kheirmand, H. Gharibi, R.A. Mirzaie, M. Faraji, M. Zhiani, J. Power Sources 169 (2007) 327.
[27] L. Genies, Y. Bultel, R. Faure, R. Durand, Electrochim. Acta 48 (2003) 3879.